JOURNAL OF AIRCRAFT
Vol. 40, No. 1, January–February 2003

Investigation of Support Interference in High-Angle-of-Attack Testing

G. S. Taylor* and I. Gursul†
University of Bath, Bath, England BA2 7AY, United Kingdom
and
D. I. Greenwell‡
QinetiQ, Bedford, England MK41 6AE, United Kingdom

An investigation was undertaken to understand support interference in high-angle-of-attack testing with particular emphasis on premature vortex breakdown induced by struts. In static experiments efforts concentrated on the support geometry and its location with respect to leading-edge vortices generated by delta wings. Extensive flow visualization studies show that vortex breakdown induced by a dummy support might move over the wing depending on the angle of attack and the location of the support. As the lateral distance between the vortex axis and support is varied, static hysteresis of vortex breakdown location was observed, which will have very important implications on force measurements in wind-tunnel testing. The results also suggest that support interference is more important for slender wings. To separate the effects of time-dependent vortex strength and support interference, the model was kept stationary, and a dummy support was oscillated in the spanwise direction in the oscillatory experiments. It was observed that vortex breakdown location oscillates with large amplitudes at low frequencies, but does not show any response at high frequencies, indicating that the frequency response is similar to that of a low-pass filter. Variation of phase-averaged breakdown location showed hysteresis loops and time lags, which are larger for a thin flat plate than a circular cylinder. The results suggest that support interference problems are more complex in transient experiments.

Introduction

STATIC support interference becomes a particular problem when testing aircraft models at high angles of attack where there are vortices originating from forebodies, wings, strakes, and canards. Support systems interfere with the vortices and wakes shed from the model. Hummel[1] demonstrated how the support interference could affect the vortices and cause premature vortex breakdown. An obstacle placed one chord length downstream of the trailing edge of a delta wing caused the vortex breakdown to move from 80 to 40% of the chord length, hence changing the wing loading. The "obstacle" used by Hummel had a relatively large projection (crossflow) area and was not representative of struts used in wind-tunnel testing. Nevertheless, his experiments indicated the potential adverse effects that might be encountered in high incidence experiments. One expects that the degree of the support interference depends on the size of the support as well as the vortex strength and trajectory, which are functions of angle of attack, roll angle, and sideslip angle. There are no available data in the literature that can be used to predict the degree of support interference.

Dynamic support interference is a bigger problem because the support structure is much bulkier than in a static test. Several studies pointed out the importance of support interference in dynamic testing, in particular premature vortex breakdown caused by the presence of struts in model aircraft wakes.[2–5] The DERA oscillatory dynamic testing facility with C-strut is shown in Fig. 1. According to Ericsson and Reding,[3] this type of curved struts as well as other rotary rigs used by NASA are typical examples of support interference in high-angle-of-attack dynamic testing. Again there are no available data in the literature that can provide a basic understanding of the extent of dynamic support interference and that can also be used as a design guide to decrease the support interference. Also, in dynamic testing the interaction of vortices with the support structure becomes more complex because the strength and trajectory of the vortices are time dependent. In addition, frequency of the model motion is an important parameter that determines the dynamic response of vortex breakdown. It is necessary to separate the effects of dynamic support interference and time-dependent vortex strength on vortex breakdown.

The main objective of this project is to increase our understanding of the support interference problem in oscillatory dynamic testing with particular emphasis on vortex breakdown. Even very basic issues such as the effect of support geometry and location, amplitude and frequency of model motion are not understood. As already discussed, the time dependency of vortex strength and trajectory in dynamic testing significantly complicates the analysis of support interference. To separate the effects of time-dependent vortex strength and support interference, it was decided to keep the model stationary and oscillate a dummy support in the spanwise direction. Hence vortex strength remained constant as there was no movement of the model, allowing a simplified analysis of dynamic support interference effects. In this paper extensive flow visualization studies are reported from static, oscillatory, and transient experiments conducted in a water tunnel to document the interference effects on vortex breakdown.

Experimental Setup

Experiments have been performed in a free-surface water tunnel (Eidetics Model 1520) with a 0.381×0.508 m working section. The tunnel can achieve speeds in the range 0 to 0.45 m/s through a closed-circuit continuous flow system. The tunnel has four viewing windows: three surrounding the test section and one downstream allowing axial viewing. The height of the test section above the floor allows flow visualization from below as well as from the sides. The water tunnel has a horizontal working section, and models have been mounted upside down, as shown in Fig. 2a. Models supported with a vertical strut underneath the wing surface are used in the

Received 3 March 2002; revision received 23 September 2002; accepted for publication 24 September 2002.

*Postgraduate Student, Department of Mechanical Engineering.
†Reader, Department of Mechanical Engineering. Member AIAA.
‡Technical Specialist; currently University of Bristol, Department of Aerospace Engineering.

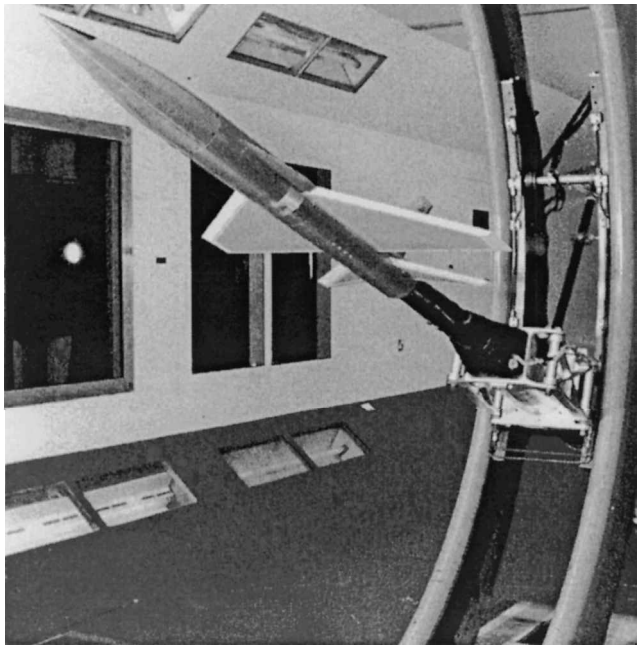

Fig. 1 DERA Unsteady Aerodynamics Testing Facility.

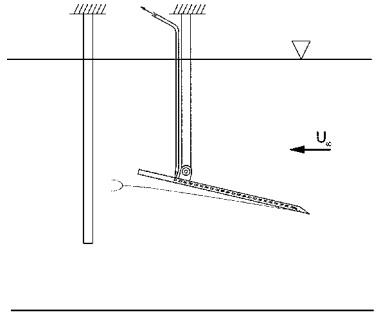

Fig. 2a Schematic of the water tunnel and model.

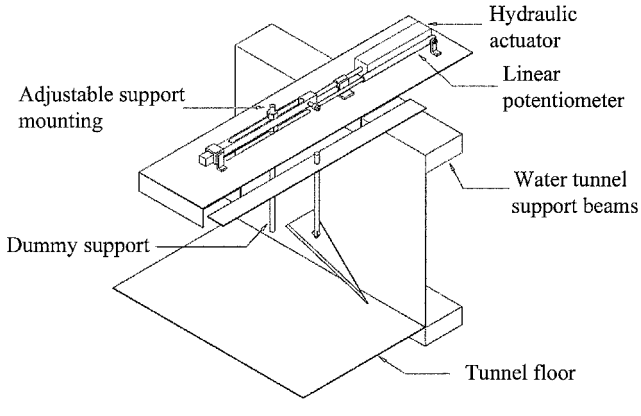

Fig. 2b Schematic of oscillating dummy support rig and model.

water-tunnel experiments so that any unwanted interference with the leading-edge vortices is minimized. A single dummy strut is placed downstream in the wake of the model wings, as also shown in Fig. 2a. In the initial experiments only the static case was considered by placing the dummy support at fixed locations downstream of the model.

A schematic of the setup for the dynamic dummy support is shown in Fig. 2b. Oscillation of the dummy support in the spanwise direction was achieved by mounting a hydraulic actuator above the water tunnel. The actuator piston was rigidly connected to a square-sectioned beam through which a vertical slot was machined; the support was bolted through this slot. The actuator piston and cross beam ran through two guides fixed rigidly to the base plate to ensure

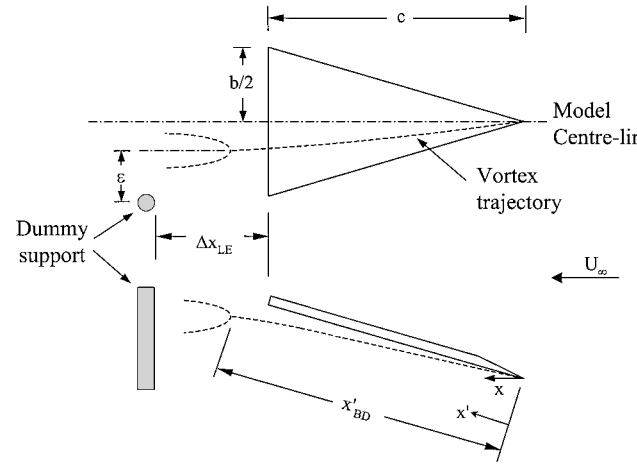

Fig. 3a Overview of experimental setup.

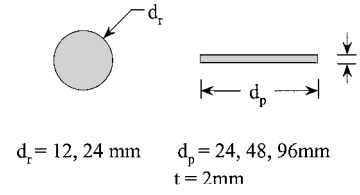

Fig. 3b Dummy support dimensions.

motion of the support was along a single axis only. Motion of the support was controlled via a desktop PC using a Data Translation DT21EZ data-acquisition card with 12-bit D/A conversion; analog output from the card was taken to a valve drive amplifier utilizing feedback control to position the support accurately. The feedback signal was output from a linear potentiometer connected at one end to the base plate and the other to the actuator piston. HP-VEE data-acquisition software was used to generate different waveforms (oscillatory and transient) to control the oscillation of the support remotely from the PC. The maximum operating frequency of the rig was approximately 0.5 Hz, being limited by the size of the hydraulic pump.

Experiments were conducted with simple delta wings with sweep angles $\Lambda = 70$, 75, 80, and 85 deg. Angles of attack up to 40 deg were considered in the experiments. The chord lengths of the model wings varied from $c = 0.137$ to 0.285 m. The thickness of the delta wings was 5 mm. For all wings the lee surface was flat, whereas the leading edges were beveled at 45 deg on the windward side. The freestream velocity was $U_\infty = 0.1$ m/s, giving Reynolds numbers in the range of $Re = 1.2 \times 10^4 - 2.5 \times 10^4$.

The effect of the dummy support on vortex breakdown location was studied by placing the support at one of three downstream locations. The location of the support was defined by ΔX_{LE} (see Fig. 3a) and took the value c, $c/2$, and $c/4$. At each of these downstream locations, the vortex breakdown location was measured for a range of values of ε/b, where ε/b is the nondimensional spanwise distance between the vortex core and the centerline of the dummy support (ε is positive outboard; see Fig. 3a). In addition to the effect of dummy support location, the effect of support cross section was also considered. Five different dummy supports have been used, being two of circular section and three of rectangular section. Figure 3b shows the dummy support dimensions used.

Dye flow visualization is used to visualize the vortex trajectories and breakdown location. Food-coloring dye diluted 1:4 with water is used to mark the vortex core. To facilitate dye flow visualization, dye tubes with an internal and external diameter of 0.81 and 1.02 mm were embedded in the lower surface (pressure side) of the models, exiting just aft of the wing apex. Pressurized dye canisters with flow control valves were used to force dye through the tubing. Dye canisters were connected to the wing tubing by using plastic tubes of a similar diameter. To ensure that the dye itself did not affect the formation of the vortices over the leading edges, the exit velocity

was carefully controlled. A digital video camera was used to record the flow visualization and to further analyze the results. A Panasonic NV DS99B digital video camera with a capture rate of 25 frames per second, a variable exposure time of 1/50 to 1/250 s, and a resolution of 570,000 pixels was used to capture images. The camera was interfaced to a desktop computer via a Pinnacle Systems StudioDV digital video capture board, which allows real-time viewing and capture of camera images.

The measurement uncertainty of the breakdown location from a single image was about $0.01c$. The time-averaged breakdown location was visually estimated from long records of flow visualization. In a few cases ($\alpha = 30$, 35, and 40 deg for $\Lambda = 80$ deg), the video recording of the motion was analyzed frame by frame to obtain the time history of breakdown location. The rms value of the fluctuations of breakdown location was determined from these time histories. At $\alpha = 30$ deg a typical value of the rms value of breakdown location was around $(X'_{BD})_{rms}/c \cong 0.035$, which is in close agreement with a previous study.[6] At higher incidence, $\alpha = 40$ deg, the rms value of the fluctuations was $(X'_{BD})_{rms}/c \cong 0.017$ and 0.027 for support-induced premature breakdown and natural breakdown, respectively.

Flowfield measurements were carried out by a particle image velocimetry (PIV) system in absence of a dummy support in order to document the properties of the undisturbed vortex. The PIV system utilized a pair of 30-mJ Nd:YAG lasers with a TSI PIVCAM 10-30 camera (operating at 30 frames per second, giving 15 measurements per second in cross correlation). The software Insight was used to postprocess the data. The flow was seeded with Polyamid particles of mean diameter of 50 μm and a density of 1.03 gr/cm^3, making them slightly less than neutrally buoyant. The 80-deg delta wing was set at angle of attack of 30 deg with a freestream velocity of 10 cm/s. The laser sheet was placed at the trailing edge and at one-quarter, one-half, and one chord length downstream of the trailing edge. The crossflow velocity field at these stations was measured by illuminating the plane from below. The crossflow plane was viewed by the camera placed near the downstream viewing window.

Results

Support Interference in Static Experiments

Figure 4 demonstrates how the location of the vortex breakdown is affected by the presence of a dummy support located at one-quarter chord downstream of the model ($\Delta X_{LE}/c = 0.25$) at $\alpha = 20$, 25, and 30 deg for the delta wing with $\Lambda = 80$ deg. In these pictures the support is located at $\varepsilon = 0$ (i.e., in line with the vortex core). It is clearly seen that in each case the presence of the support induces vortex breakdown upstream of the support, compared with the control case where no breakdown is observed. The largest angle of attack ($\alpha = 30$ deg) seems to produce the most dramatic changes

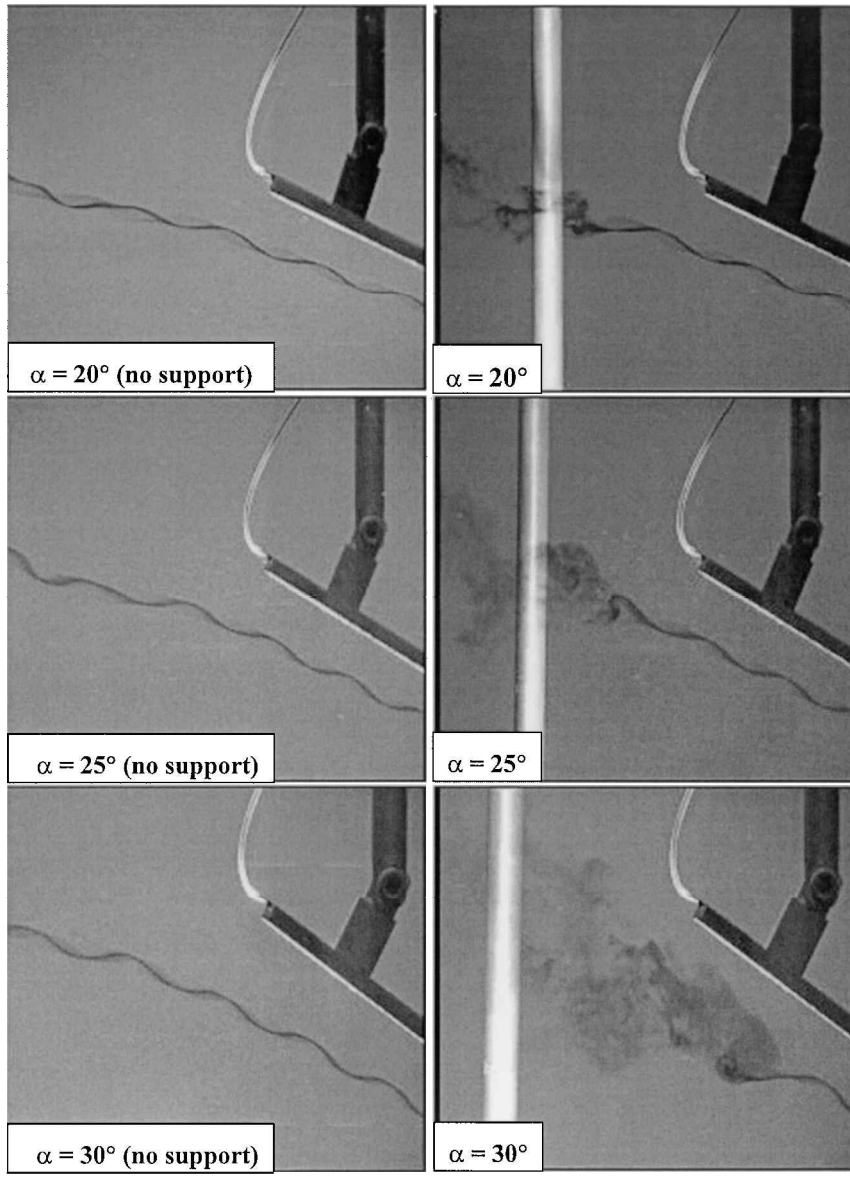

Fig. 4 Variation of vortex breakdown location with angle of attack for 80-deg delta, with dummy support set at $\Delta X_{LE}/c = 0.25$.

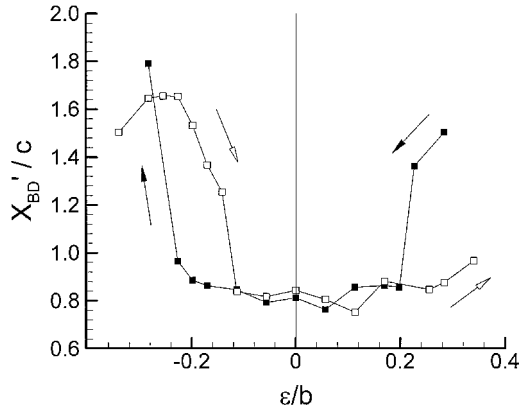

Fig. 5 Variation of time-averaged breakdown location as a function of normalized spanwise location of the dummy support: $\Lambda = 80$, $\alpha = 30$ deg, and $\Delta X_{LE}/c = 0.50$, for the cylindrical support $d = 12$ mm.

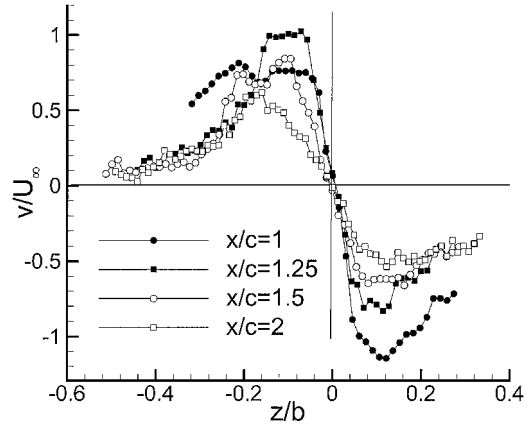

Fig. 6 Variation of normalized horizontal component of velocity with vertical distance from the vortex core: $\Lambda = 80$ deg and $\alpha = 30$ deg.

in the presence of the dummy support. Hence detailed studies were carried out for this incidence. Figure 4 also demonstrates that the location of this induced breakdown is dependent on the angle of attack of the delta wing, and therefore upon the condition of the vortex.

To study the effect of spanwise (lateral) location of the dummy support for $\alpha = 30$ deg, the support was first located at a lateral position away from the model centerline, where no effect on the vortex was observed. The support was then stepped towards the vortex core, and the vortex breakdown location was recorded. The support was moved in both directions, corresponding to increasing and decreasing ε values. Figure 5 shows the variation of the time-averaged breakdown location as a function of ε/b for 30-deg incidence, $\Delta X_{LE}/c = 0.50$ and the cylindrical support with diameter $d = 12$ mm. It is seen that for decreasing ε the vortex breakdown first appears in the wake ($X'_{BD}/c \cong 1.5$) when $\varepsilon/b \cong 0.3$. As ε is decreased to around $\varepsilon/b \cong 0.2$, the breakdown moves over the wing and stays around nearly the same location with further decreases in ε. For negative values of ε as it is decreased, there is nearly symmetric response of vortex breakdown. However, when the same experiment is repeated in the opposite direction (increasing ε) some asymmetry is observed, in particular in the width of the plateau near $\varepsilon = 0$. Nevertheless, the main features for increasing and decreasing ε are the same. Therefore it was decided to continue with further experiments for $\varepsilon \geq 0$ only.

Before studying the effect of different parameters such as streamwise location and cross section of the dummy support, it was decided to document the undisturbed vortex flow in detail for $\alpha = 30$ deg. The PIV measurements were performed at the trailing edge and at a quarter-chord, a half-chord, and one chord length from the trailing edge in the absence of the dummy support. The detailed time-averaged crossflow velocity field is presented in Ref. 7. The leading-edge vortex pair is fairly symmetric and coherent with no signs of vortex breakdown for the undisturbed flow (in the absence of the dummy support) within one chord length distance from the trailing edge. Variation of the normalized horizontal component of velocity with vertical distance from the vortex core is shown in Fig. 6. The initial asymmetry of the velocity profile within the vortex at the trailing edge (because of the wing surface) more or less disappears at one-quarter chord length from the trailing edge. The maximum swirl velocity decreases with increasing streamwise distance while the vortex core radius increases from $r_0/b \approx 0.05$ to 0.15. The calculated circulation of the vortices was roughly constant in the wake.[7] The maximum circulation measured at the trailing edge $\Gamma/U_\infty c \cong 0.40$ is close to the measured value for a similar wing ($\Gamma/U_\infty c \cong 0.37$) at much higher Reynolds numbers in a wind tunnel.[8]

Figures 7–9 show how the vortex breakdown location varies with the lateral support location at $\Delta X_{LE} = c$, $c/2$, $c/4$ for three dummy support configurations. Detailed results for all five dummy supports were reported previously.[7] All of these experiments were performed

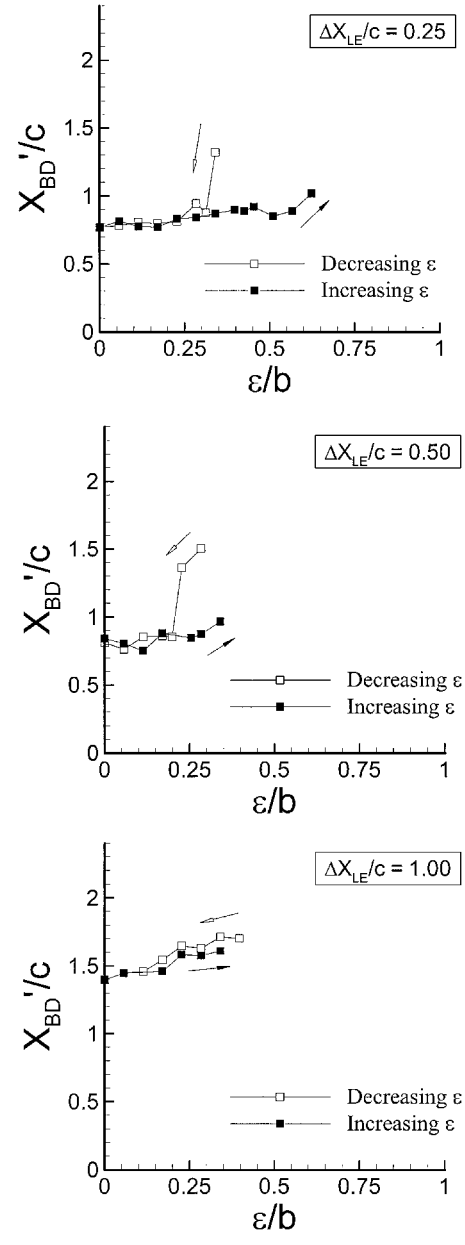

Fig. 7 Variation of vortex breakdown location with spanwise location of the support for 12-mm rod.

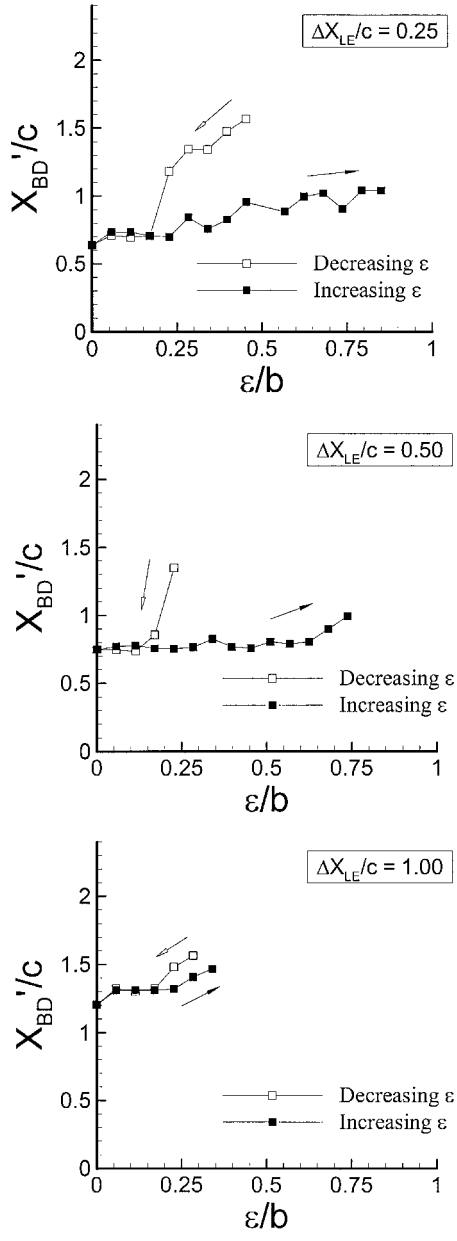

Fig. 8 Variation of vortex breakdown location with spanwise location of the support for 24-mm rod.

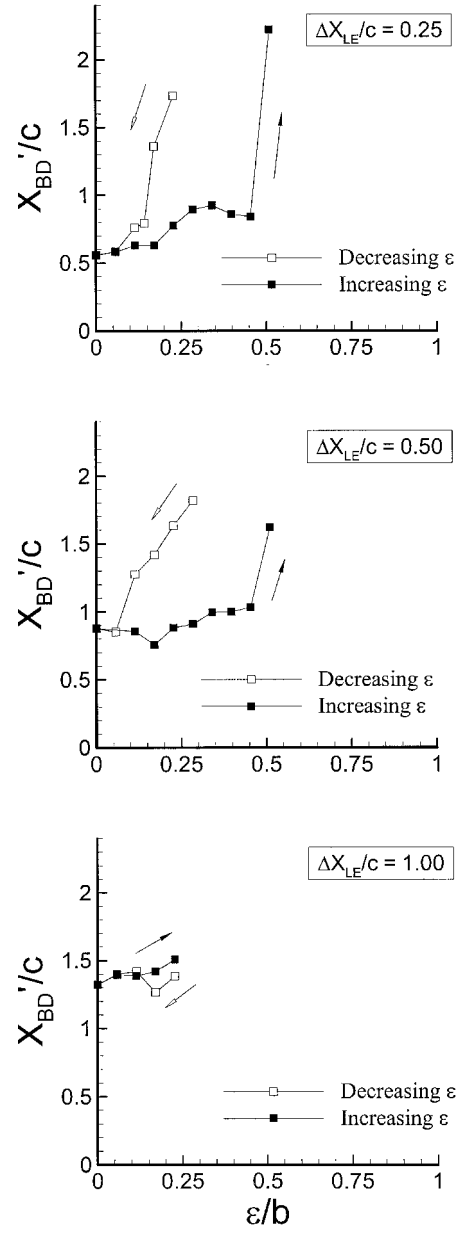

Fig. 9 Variation of vortex breakdown location with spanwise location of the support for 96-mm plate.

at $\alpha = 30$-deg incidence. In each test the support was started at a point at which no influence on the vortex was observed and stepped towards the center of the vortex. Once reaching the vortex centreline ($\varepsilon = 0$), the reverse procedure was followed. The direction in which each data set was taken is shown on the plots. Figure 7 (top) shows the influence of a 12-mm rod set at one-quarter chord downstream of the trailing edge of the delta. When the support is moved from outside of the vortex towards the vortex core, breakdown is induced when the support reaches $\varepsilon/b \cong 0.35$, but more importantly breakdown is observed upstream of the trailing edge ($X'_{\mathrm{BD}}/c < 1$) when $\varepsilon/b \cong 0.30$. However, in the reverse case, when the support is moved away from the vortex core, the vortex breakdown is observed until $\varepsilon/b \cong 0.60$. This phenomenon is observed for all of the cross sections so far considered and indicates that the vortex has a preference to remain in its current state. For instance, when there is no breakdown the dummy support needs to be located close to the vortex core before vortex breakdown is observed, but when already broken the dummy support needs to be moved farther away than was first necessary to achieve breakdown before the vortex returns to its original undisturbed state.

This static hysteresis effect is reduced as the dummy support moved further downstream as shown in Fig. 7. In fact, the seeming preference of the vortex to remain in its current state appears to hold more when the breakdown occurs forward of the trailing edge of the delta wing. In the cases where breakdown is observed aft of the trailing edge ($X'_{\mathrm{BD}}/c > 1.0$), the hysteresis effect is vastly reduced as shown in Fig. 9.

Figures 7–9 clearly show that the worst case of support interference (i.e., when the vortex breakdown occurred most forward) was in all cases when the dummy support was located in line with the vortex core ($\varepsilon/b = 0$) and was at its closest to the trailing edge of the delta wing ($\Delta X_{\mathrm{LE}} = c/4$). Increasing the diameter of the cylindrical support caused earlier breakdown and widened the region over which the hysteresis was observed, as shown in Fig. 8. When plates were used for the dummy support, there was little to separate the 24- and 48-mm plate results,[7] whereas the 96-mm plate appeared to be the worst support of all, as it pushed the breakdown further forward than any of the other supports (see Fig. 9). Also, the hysteresis region was wide in this case. These results show that a thin cross section is not necessarily desirable if the length in the streamwise direction is large. In other words, streamlined supports might not be as good as those with a circular cross section. It is postulated that this effect is caused by the boundary condition imposed on the azimuthal velocity component of the vortical flow.

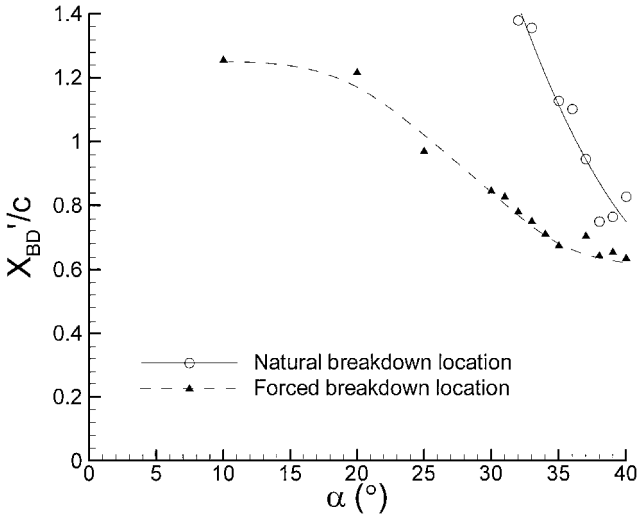

Fig. 10 Variation of breakdown location for natural and forced cases (for $\Delta X_{LE}/c = 0.25$, $\varepsilon/b = 0$, and $d = 12$ mm) as a function of angle of attack: $\Lambda = 80$ deg.

With regard to the static hysteresis behavior of vortex breakdown observed in these experiments, several investigators noted similar observations when the angle of attack is varied (for example, see Lowson[9]). For a $\Lambda = 80$-deg sweep delta wing Lowson reported that vortex breakdown appears near the trailing edge at $\alpha = 41$ deg when α is increased, but remains over the wing until α is decreased to 34 deg. Tobak and Peake[10] suggested that the static hysteresis can be explained as a subcritical bifurcation of vortex flows over slender wings at high angle of attack. They note that subcritical bifurcation of three-dimensional separated flows always leads to hysteresis effects. Nonuniqueness and hysteresis of vortex breakdown were also noted in several theoretical and numerical studies[11–13] when the swirl level is varied in various axisymmetric cases and in delta wing flows[14] when angle of attack is varied. According to Visbal,[14] static hysteresis of vortex breakdown was computed even for relatively lower sweep angles such as $\Lambda = 65$ deg. Previous studies found the static hysteresis as the strength of the vortices is varied. In contrast, in this study the delta wing is stationary and fixed at a given angle of attack; therefore, the strength is not a variable. Yet, as the location of the dummy support is varied the hysteresis is observed.

The effect of angle of attack was investigated in detail for the cylindrical support with $d = 12$ mm. In these experiments the location of the dummy support is fixed at $\Delta X_{LE}/c = 0.25$, and the direct impingement of the vortex was considered ($\varepsilon = 0$) as this represents the most adverse conditions for the support interference. The variation of breakdown location is shown as a function of angle of attack in Fig. 10 for $\Lambda = 80$ deg. Also, the data points are shown for the natural case (in the absence of the support) for comparison. At low angles of attack, the vortex breakdown location is just upstream of the dummy support (for example, see $\alpha = 20$ deg in Fig. 4) and downstream of the trailing edge of the wing. As the angle of attack is increased, vortex breakdown location appears at the trailing edge for $\alpha \cong 25$ deg, whereas in the natural case it appears at the trailing edge for $\alpha \cong 36$ deg. At large angles of attack, the data for the natural and induced breakdowns have a trend of merging. Hence there seem to exist two plateaus, one at low angles of attack and the other one at large angles of attack. In between these regions, vortex breakdown is very sensitive to the presence of the dummy support, and largest deviations from the undisturbed case are found in this region. It is suggested that the leading-edge vortex reaches a critical stage in this region.

The effect of sweep angle can be seen in Fig. 11, where the variation of breakdown location with incidence is shown for $\Lambda = 70$, 75, 80, and 85 deg. The difference between the forced and natural cases is small for $\Lambda = 70$ deg, but increases with increasing sweep angle. Hence, the results suggest that support interference might be more

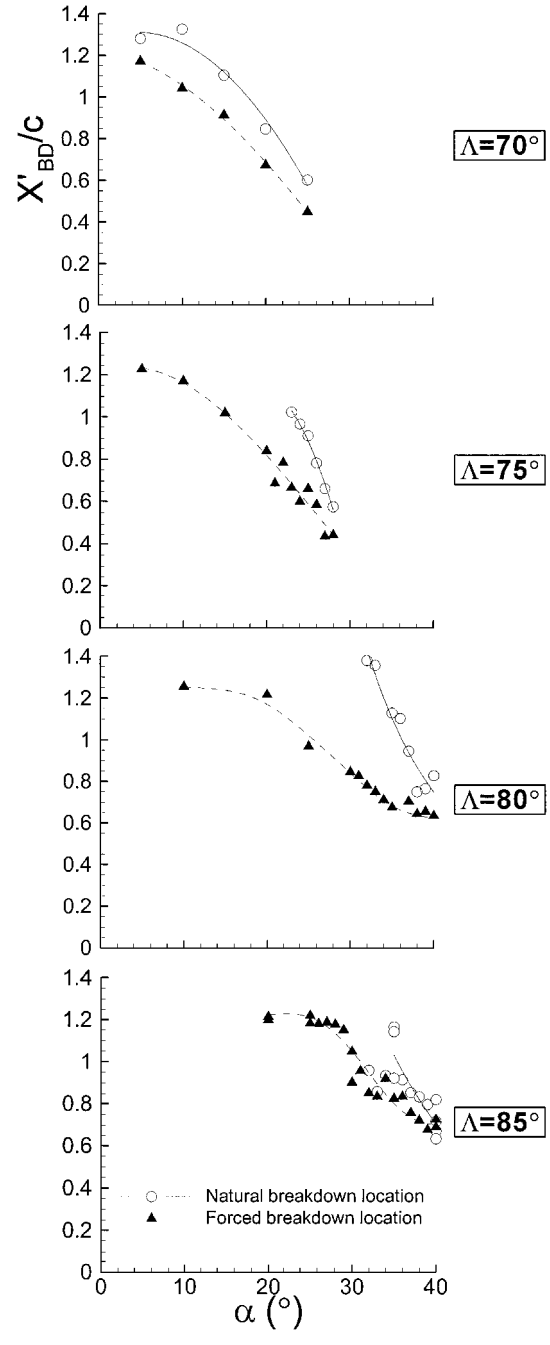

Fig. 11 Variation of breakdown location with incidence for natural and forced cases (for $\Delta X_{LE}/c = 0.25$, $\varepsilon/b = 0$, and $d = 12$ mm).

important for slender wings. Some comparison of the present results for the natural case is made with the data collected by Erickson,[15] who showed that the angle of attack at which breakdown appears at the trailing edge differs considerably (as much as 10 deg) in different facilities. In fact, the scatter of vortex breakdown location data is largest near the trailing edge.[16] Lowson and Riley[17] demonstrated that detailed model geometry is the most important factor for the scatter of the data, and other effects such as support interference and Reynolds number are secondary. The present data for $\Lambda = 70$ and 75 deg are near the lower end of the reported range, whereas the data for $\Lambda = 80$ and 85 deg are near the middle of the range. Figure 11 shows that the results for the sweep angle $\Lambda = 85$ deg do not appear to confirm the increasing trend of the data for the natural case. This is similar to the results of Wentz and Kohlman,[18] who showed that for large sweep angles the breakdown occurs at a constant angle of attack (around 38 deg), independent of sweep. Finally, although nonslender wings seem to be much less vulnerable

to support interference problems at zero sideslip angle they might be more sensitive at nonzero sideslip angles. It was shown in Ref. 7 that as the sideslip angle was varied for $\Lambda = 70$-deg wing the vortex reached a critical stage, even at low angles of attack such as 15 deg, leading to a large difference between the forced and natural cases.

Support Interference in Oscillatory Experiments

In the oscillatory experiments location of the dummy support was varied periodically according to

$$\varepsilon = \varepsilon_0 + \varepsilon_1 \cos \omega t = \varepsilon_0 + \varepsilon_1 \cos 2\pi f_e t \qquad (1)$$

The mean location was varied in the range $\varepsilon_0/b = 0$–0.3, and the amplitude was varied between $\varepsilon_1/b = 0.1$ to 0.285. The reduced frequency $f_e c/U_\infty$ was in the range of 0.025–0.5. All of the flow visualization experiments were carried out at an incidence of $\alpha = 30$ deg for $\Lambda = 80$-deg delta wing and $\Delta X_{LE}/c = 0.25$. An example of time histories of breakdown location is shown in Fig. 12 for a 96-mm plate, $\varepsilon_0/b = 0.285$, $\varepsilon_1/b = 0.285$ at different reduced frequencies. It is seen that the amplitude of the fluctuations of breakdown location is very large for the smallest reduced frequency $f_e c/U_\infty = 0.025$, but becomes smaller rapidly with increasing frequency. The vortex breakdown does not respond much to the oscillations of the dummy support at high frequencies. Hence, it is confirmed that the frequency of the motion is a very important parameter.

The effect of the excitation frequency can also be seen from the amplitude of the cross spectrum between location of vortex breakdown and motion of support in Fig. 13 for the same parameters as those in Fig. 12. In each spectrum the excitation frequency of the dummy support motion is shown with an arrow. For the smallest excitation frequency $f_e c/U_\infty = 0.025$, a very large spectral amplitude is observed at the excitation frequency. It is seen that the peak spectral amplitude decreases with increasing excitation frequency. These observations suggest that the response of breakdown location

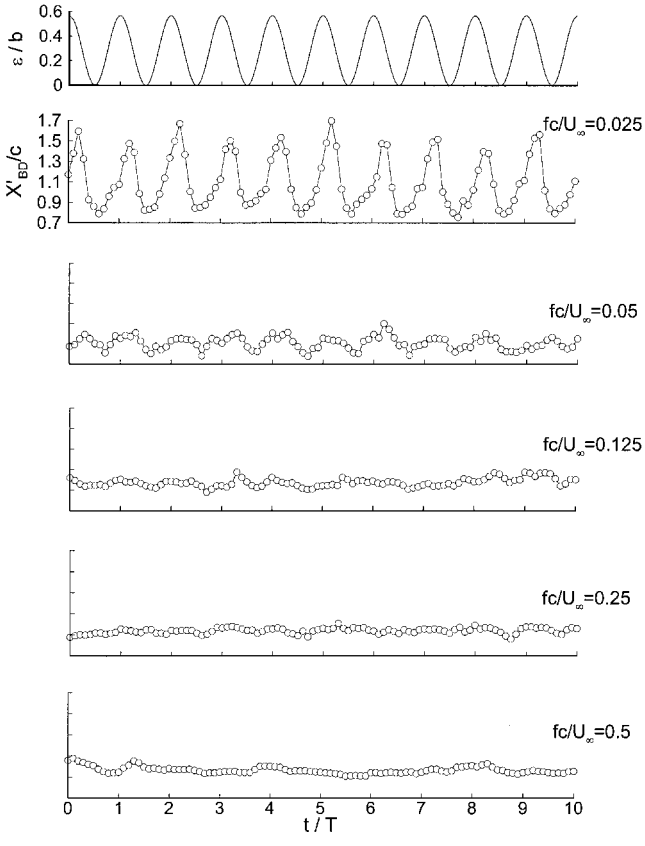

Fig. 12 Time history of breakdown location for different oscillation frequencies of the dummy support for 96-mm plate: $\Delta X_{LE}/c$ = 0.25, ε_0/b = 0.285, and ε_1/b = 0.285.

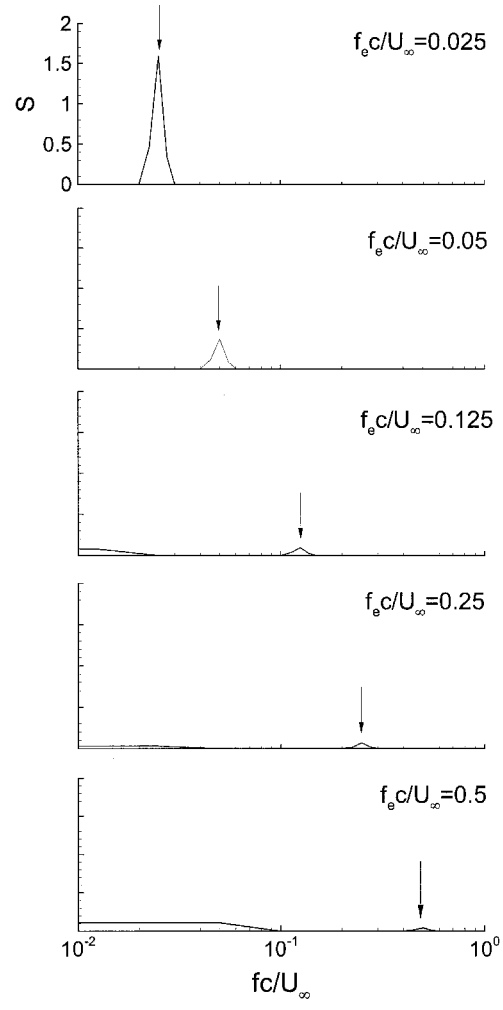

Fig. 13 Spectra of breakdown location for different oscillation frequencies of the dummy support for 96-mm plate: $\Delta X_{LE}/c$ = 0.25, ε_0/b = 0.285, and ε_1/b = 0.285.

is similar to that of a low-pass filter. Similar behavior of vortex breakdown was reported recently[19] for an oscillating fin near the trailing edge of a delta wing. It was also shown that the frequency response of breakdown location in different unsteady flows (such as for pitching delta wing, oscillating fin, etc.) is similar, suggesting a common, universal mechanism, regardless of the unsteady motion.[20] A mechanism based on the wave propagation characteristics of the vortex flows was proposed to explain the experimental observations. The present study shows that observations in the near wake caused by an oscillating dummy support ($\Delta X_{LE}/c = 0.25$) are similar to those on the wing in previous studies. An analytical model that predicts the frequency response of vortex breakdown location has been recently proposed.[21]

Figure 14 shows the variation of the peak spectral amplitude as a function of forcing frequency for different amplitudes and 96-mm plate as well as 12-mm rod. As long as the amplitude of the fluctuations of breakdown location is not too small, the results for both large- and small-amplitude cases are qualitatively similar, confirming the effect of reduced frequency on the response of breakdown location. Although only the peak spectral amplitude is shown in Fig. 14, it is evident that the rms value of the fluctuations of breakdown location strongly depends on the excitation frequency. Whereas the largest rms value for 12-mm rod is around 0.06c, it can be as large as 0.26c for 96-mm plate.[22]

It is interesting to examine the variation of phase-averaged breakdown location as shown in Fig. 15 for different reduced frequencies and large-amplitude motion of 96-mm plate. At the smallest reduced frequency vortex breakdown location forms a hysteresis loop when plotted as a function of dummy support location because of

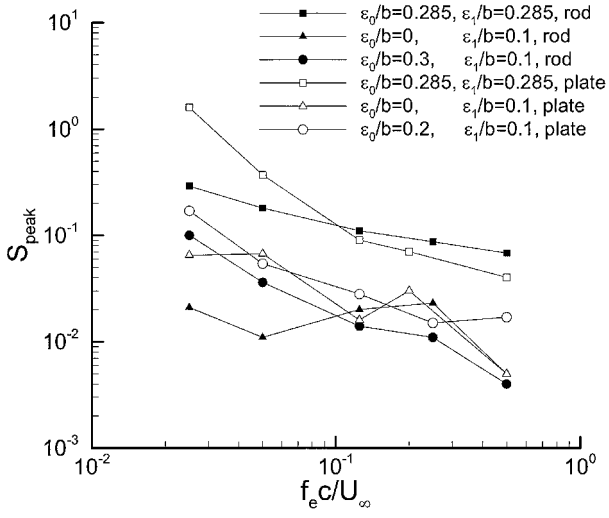

Fig. 14 Variation of peak spectral amplitude as a function of forcing frequency for different oscillatory motions.

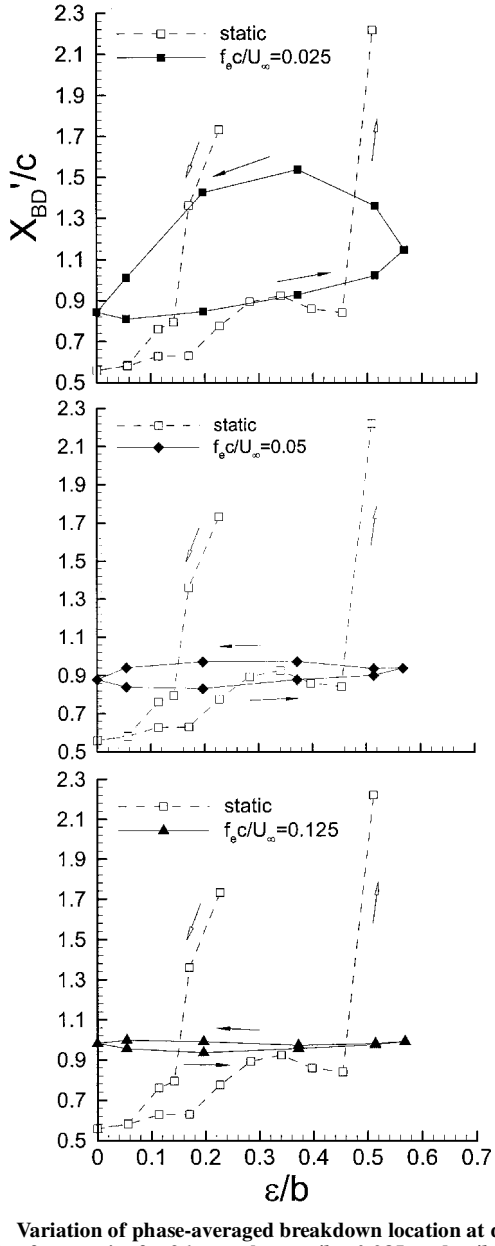

Fig. 15 Variation of phase-averaged breakdown location at different oscillation frequencies for 96-mm plate: $\varepsilon_0/b = 0.285$, and $\varepsilon_1/b = 0.285$.

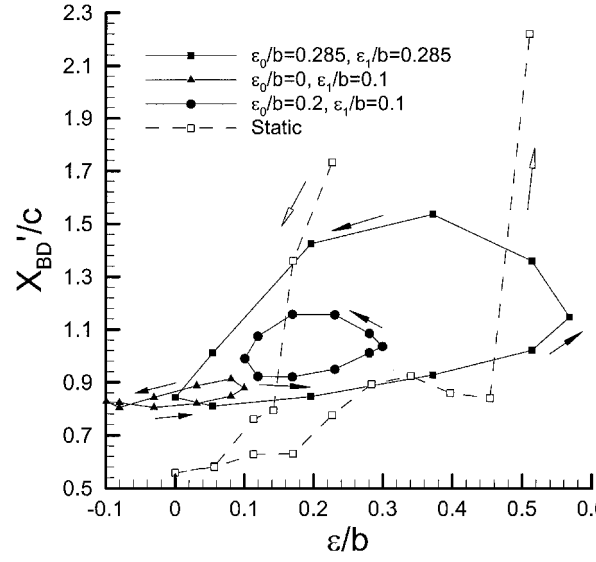

Fig. 16 Variation of phase-averaged breakdown location for different amplitudes of oscillatory motion for 96-mm plate and $f_e c/U_\infty = 0.025$.

the time lag of breakdown location (with respect to the displacement of the dummy support). Note that the dynamic hysteresis loop does not cause large variations in breakdown location as much as static hysteresis does. With increasing frequency the dynamic hysteresis loops flattens, as vortex breakdown does not respond to the motion of the dummy support and its location becomes roughly constant. Although not shown here but reported in Ref. 22 in detail, the hysteresis loop is much narrower for the rod, which indicates smaller time lag of breakdown location. The cross-spectral analysis of location of vortex breakdown and motion of the dummy support revealed that the phase lag at $f_e c/U_\infty = 0.025$ is $\phi = 61$ and 47 deg for 96-mm plate and 12-mm rod, respectively.

Figure 16 shows the effect of different amplitudes of oscillatory motion for 96-mm plate at a fixed reduced frequency $f_e c/U_\infty = 0.025$. The large-amplitude case causes large hysteresis effect and an unexpected delay in the time-averaged value. Even for small-amplitude cases, the effect is larger when the motion of the support covers sensitive regions in the static case. For example, the case of $\varepsilon_0/b = 0.2$ and $\varepsilon_1/b = 0.1$ shown in Fig. 16 has considerable hysteresis, compared to $\varepsilon_0/b = 0$ case. Again, the hysteresis loops and corresponding time lags are larger for the plate than the rod.[22]

Support Interference in Transient Experiments

Several different waveforms for the transient experiments were considered. Time history of the motion of the dummy support for different transient cases studied is shown in Fig. 17. These include various sinusoidal single full-wave motions of different amplitudes (cases A–D), half-wave motion corresponding to the dummy support cutting through the vortex axis (case E), and dummy support moving to $\varepsilon = 0$ and stopping (case F). In each case the characteristic period of the single full/half-wave was varied.

Two important observations were made during these transient experiments. First, there was an increasing time delay in the first appearance of the vortex breakdown. This is shown in Fig. 18 for case F, where time histories of breakdown location for different nondimensional frequencies are shown for 12-mm rod. The first data point in each case corresponds to the first appearance of vortex breakdown. It is seen that there is substantial delay in the occurrence of breakdown at high frequencies. Another piece of information that can be obtained from Fig. 18 is an estimate of the time constant for the motion of vortex breakdown. The normalized time constant $\tau U_\infty/c$ is around 2.5, which is consistent with previously reported values for various unsteady vortex flows.[23,24]

The second important observation is that the minimum breakdown location (corresponding to its most upstream location) strongly depends on the nondimensional frequency of the motion.

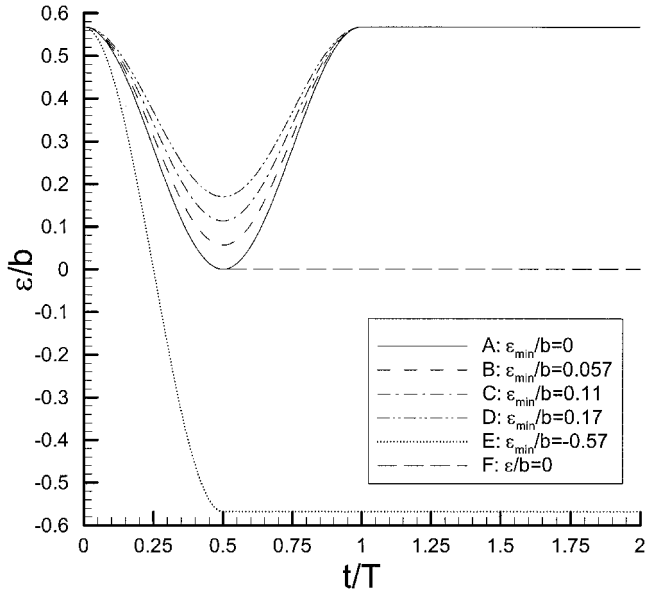

Fig. 17 Time history of dummy support motion for several transient cases studied.

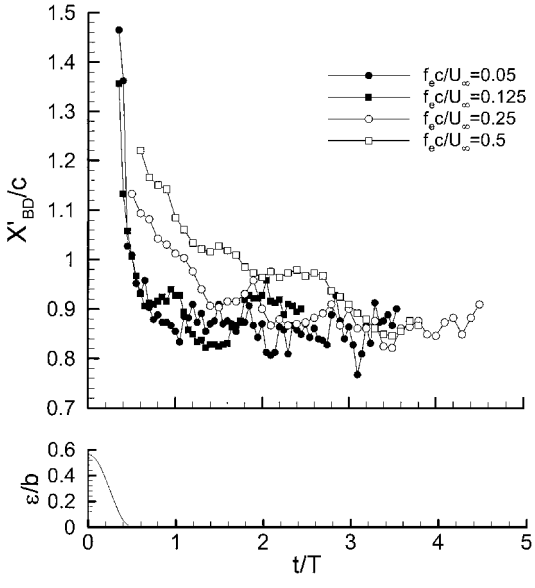

Fig. 18 Response of vortex breakdown location to transient motion of dummy support for different nondimensional frequencies.

This is illustrated for 12-mm rod in Fig. 19 for case A (where the minimum ε is zero), and the pictures are taken for $\varepsilon = 0$ at different frequencies. It is seen that vortex breakdown is most upstream for the smallest frequency and is further downstream with increasing frequency. In fact, there is no clearly identified breakdown upstream of the dummy support at the highest frequency, although there is strong interaction of the vortex with the support and consequent deformation of the vortex core. For various transient motions (cases A–E) of different amplitudes and frequencies, it was noticed that the minimum breakdown location is a strong function of the static hysteresis characteristics. For the 12-mm rod vortex breakdown is observed first at $\varepsilon/b = 0.32$ for decreasing ε in the static experiments (see Fig. 7). For various transient motions the parameter τ_C is defined as the length of time during which $|\varepsilon/b| < 0.32$. This parameter is plotted in Fig. 20 as a function of the minimum breakdown location. It is seen that there is a good correlation between this parameter and minimum breakdown location.

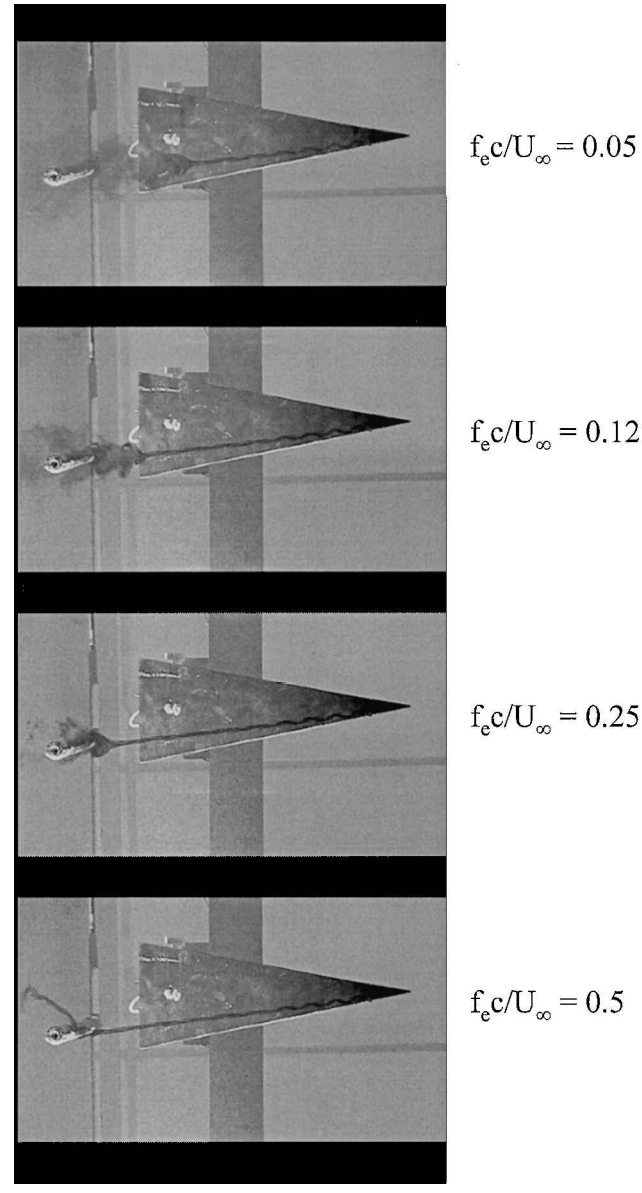

Fig. 19 Flow visualization of the interaction of leading-edge vortex with the dummy support for transient motion with different nondimensional frequencies.

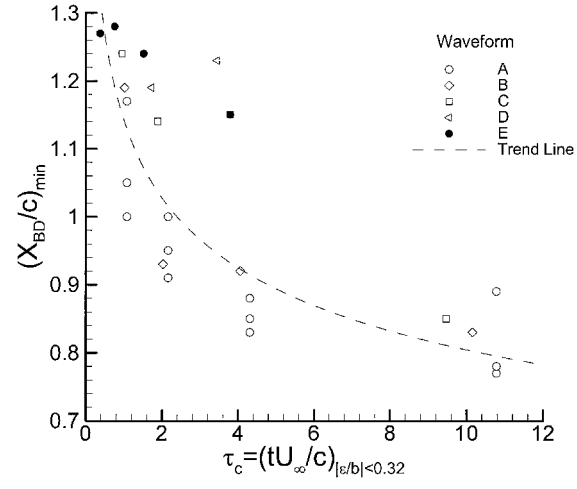

Fig. 20 Variation of minimum breakdown location with time support spends in "region of influence" for various transient motions.

Conclusions

An investigation was undertaken to understand support interference in high-angle-of-attack testing with particular emphasis on premature vortex breakdown induced by struts. In static experiments efforts concentrated on the support geometry and its location with respect to leading-edge vortices generated by delta wings. Extensive flow visualization studies showed that vortex breakdown induced by a dummy support can move over the wing depending on the angle of attack and the location of the support. As the lateral distance between the vortex axis and support is varied, static hysteresis of vortex breakdown location was observed, which has very important implications on force measurements in wind-tunnel testing. Static hysteresis was previously observed in experiments and computations when angle of attack of the wing is varied. It is interesting that the same effect can be generated by the location of the support for a fixed delta wing. The cross section of the support had large effects on the location of vortex breakdown and hysteresis characteristics. In particular it was noted that a streamlined support can be worse than a circular cylinder. Also, it seems that support interference might be more important for slender wings.

To separate the effects of time-dependent vortex strength and support interference, the model was kept stationary, and a dummy support was oscillated in the spanwise direction. It was found that the oscillation frequency has a very large effect on the response of vortex breakdown. It was observed that the vortex breakdown location oscillates with large amplitudes at low frequencies, but does not show any response at high frequencies, indicating that the frequency response is similar to that of a low-pass filter. Similarities to the dynamics of vortex breakdown over unsteady delta wings were noted. Variation of phase-averaged breakdown location showed hysteresis loops and time lags, which are larger for a thin flat plate than a circular cylinder. For large-amplitude oscillations of the dummy support, the location of the vortex breakdown may be very different than that of static case. Hysteresis effects are more dominant when the motion of the support covers the regions that are sensitive in the static case.

Transient experiments showed that there was a delay in the occurrence of vortex breakdown with increasing nondimensional acceleration parameter. It was found that how far upstream vortex breakdown propagates strongly depends on the nondimensional acceleration parameter as well as static characteristics. Overall the results suggest that support interference problems are more complex in transient experiments.

Acknowledgment

This work was funded by the United Kingdom Ministry of Defence, under package 07b of the Applied Research Programme.

References

[1]Hummel, D., "Untersuchungen über das Aufplatzen der Wirbel an Schlanken Delta Flugeln," *Zeitschrift fuer Flugwissenschaften*, Vol. 13, No. 5, 1965, pp. 158–168.

[2]Ericsson, L. E., and Reding, J. P., "Review of Support Interference in Dynamic Tests," *AIAA Journal*, Vol. 21, No. 12, 1983, pp. 1652–1666.

[3]Ericsson, L. E., and Reding, J. P., "Dynamic Support Interference in High-Alpha Testing," *Journal of Aircraft*, Vol. 23, No. 12, 1986, pp. 889–896.

[4]Ericsson, L. E., "Another Look at High-Alpha Support Interference in Rotary Tests," *Journal of Aircraft*, Vol. 28, No. 9, 1991, pp. 584–591.

[5]Beyers, M. E., and Ericsson, L. E., "Ground Facility Interference on Aircraft Configurations with Separated Flow," *Journal of Aircraft*, Vol. 30, No. 5, 1993, pp. 682–688.

[6]Menke, M., Yang, H., and Gursul, I., "Experiments on the Unsteady Nature of Vortex Breakdown over Delta Wings," *Experiments in Fluids*, Vol. 27, 1999, pp. 262–272.

[7]Taylor, G., Gursul, I., and Greenwell, D., "Static Hysteresis of Vortex Breakdown due to Support Interference," AIAA Paper 2001-2452, June 2001.

[8]Elliott, M. S., "An Investigation into the Wing-Rock of an 80 Degree Delta Wing," Ph.D. Dissertation, Dept. of Aeronautics, Imperial College of Science, Technology and Medicine, London, Sept. 2000.

[9]Lowson, M., "Some Experiments with Vortex Breakdown," *Journal of the Aeronautical Society*, Vol. 68, May 1964.

[10]Tobak, M., and Peake, D. J., "Topology of Three-Dimensional Separated Flows," *Annual Review of Fluid Mechanics*, Vol. 14, 1982, pp. 61–85.

[11]Beran, P., and Culick, F., "The Role of Non-Uniqueness in the Development of Vortex Breakdown in Tubes," *Journal of Fluid Mechanics*, Vol. 242, 1992, pp. 491–527.

[12]Darmofal, D., "A Study of the Mechanisms of Axisymmetric Vortex Breakdown," Ph.D. Dissertation, Dept. of Aeronautics and Astronautics, Massachusetts Inst. of Technology, Cambridge, Nov. 1993.

[13]Lopez, J. M., "On the Bifurcation Structure of Axisymmetric Vortex Breakdown in a Constricted Pipe," *Physics of Fluids*, Vol. 6, No. 11, 1994, pp. 3683–3693.

[14]Visbal, M. R., "Computational and Physical Aspects of Vortex Breakdown on Delta Wings," AIAA Paper 95-0585, Jan. 1995.

[15]Erickson, G. E., "Water-Tunnel Studies of Leading-Edge Vortices," *Journal of Aircraft*, Vol. 19, No. 6, 1982, pp. 442–448.

[16]Gursul, I., "Criteria for Location of Vortex Breakdown over Delta Wings," *The Aeronautical Journal of the Royal Aeronautical Society*, Vol. 99, No. 985, May 1995, pp. 194–196.

[17]Lowson, M. V., and Riley, A. J., "Vortex Breakdown Control by Delta Wing Geometry," *Journal of Aircraft*, Vol. 32, No. 4, 1995, pp. 832–838.

[18]Wentz, W. H., and Kohlman, D. L., "Vortex Breakdown on Slender Sharp-Edged Wings," *Journal of Aircraft*, Vol. 8, No. 3, 1971, pp. 156–161.

[19]Gursul, I., and Xie, W., "Interaction of Vortex Breakdown with an Oscillating Fin," *AIAA Journal*, Vol. 39, No. 3, 2001, pp. 438–446.

[20]Gursul, I., "Proposed Mechanism for Time Lag of Vortex Breakdown Location in Unsteady Flows," *Journal of Aircraft*, Vol. 37, No. 4, 2000, pp. 733–736.

[21]Darmofal, D., "Analysis of Unsteady Vortex Breakdown Behavior Using a Quasi-One-Dimensional Model," Massachusetts Inst. of Technology Rept., Cambridge, 2002.

[22]Taylor, G. S., "An Investigation of Support Interference in Static and Dynamic Testing," Ph.D. Dissertation, Univ. of Bath, England, U.K. (to be submitted).

[23]Greenwell, D. I., and Wood, N. J., "Some Observations on the Dynamic Response to Wing Motion of the Vortex Burst Phenomenon," *Aeronautical Journal*, Vol. 98, No. 971, Feb. 1994, pp. 49–59.

[24]Gursul, I., Srinivas, S., and Batta, G., "Active Control of Vortex Breakdown over a Delta Wing," *AIAA Journal*, Vol. 33, No. 9, 1995, pp. 1743–1745.